Hindawi
Geofluids
Volume 2021, Article ID 9926063, 12 pages
https://doi.org/10.1155/2021/9926063

Research Article

Coupled Effects of Water and Low Temperature on Quasistatic and Dynamic Mechanical Behavior of Sandstone

Zilong Zhou, Yude E, Xin Cai, and Jing Zhang

School of Resources and Safety Engineering, Central South University, Changsha 410083, China

Correspondence should be addressed to Xin Cai; xincai@csu.edu.cn and Jing Zhang; zjaimme@csu.edu.cn

Received 19 March 2021; Accepted 22 April 2021; Published 5 May 2021

Academic Editor: Dayang Xuan

The mechanical behavior of rock materials is critically affected by water and temperature. To comprehensively study the coupled effects of water saturation and low temperature on the mechanical properties of sandstone, both quasistatic and dynamic compressive tests were performed on dry and water-saturated specimens under room temperature and -60°C. The results indicated that under the same strain rate, at room temperature, the compression strength and elastic modulus of the sandstone specimen are significantly reduced when the specimen becomes water-saturated. However, at -60°C, the compression strength and elastic modulus of the dry specimen notably increase compared to that at room temperature. Interestingly, these mechanical parameters of the saturated-frozen specimen are lower than that of the dry one but slightly higher than that of the saturated specimen under room temperature. Moreover, regardless of temperature, the saturated specimens have a higher strain rate dependence in terms of strength. The dual effects of water and subzero temperature of the mechanical behavior of rock are discussed.

1. Introduction

In China, a growing number of rock engineering projects (such as mining, tunneling, and railway) are constructed and proceeded in cold regions due to demands for resources and national strategies. The air temperature regularly falls below zero degrees Celsius in cold regions, where the rocks on the ground are frozen [1]. Furthermore, in some severe cold regions, such as Tibet plateau, Great Khingan mountains, the north Xinjiang area, and Inner Mongolian plateau, the lowest air temperature even can be below 60°C [2–4]. The extremely low temperature will lead to the changes of mechanical properties of rock especially with the presence of water [5, 6]. Therefore, an in-depth understanding of the freezing effects on rock performance is crucial for the security and stability of rock engineering projects in cold regimes.

In recent years, the mechanical and deformation properties of frozen rocks have been extensively studied. For instance, Winkler [7] conducted a lot of tests on rock at subzero temperature. He found that the lower the temperature, the greater the frost heave force generated by the pore ice. Inada and Yokota [8] carried out uniaxial compression and tension tests on granite and andesite specimens after being frozen up to -160°C. They reported that at -160°C, the UCS and tensile strength of two tested rocks increase compared to that tested at room temperature. Aoki et al. [9] performed similar tests on five kinds of rock types. They however discovered that the mechanical properties of five rocks decrease in different extents after freezing. The UCS loss of rocks ranges from 20% to 70%, the loss in indirect tensile strength from 50% to 100%, and the loss in Young's modulus is about 20%. Yamabe and Neaupane [10] found that the UCS and Young's modulus decrease with the decline of temperature from 20°C to −10°C, while the UCS increases in temperature from -10°C to -20°C and Young's modulus further decreases. Moreover, Dwivedi et al. [11] conducted cracked chevron-notched Brazilian disc tests on eight kinds of rocks in temperature from -10°C to -50°C to study the temperature dependence of fracture toughness. They suggested that the fracture toughness of all tested rock types shows the negative linear relationship with temperature. Tang et al. [12] carried out triaxial compressive tests on granite specimens under -10°C to -50°C. Their test results showed that the compressive strength and cohesion of the granite are inversely proportional to temperature. The temperature of -40°C is the critical temperature below which the strength and cohesion

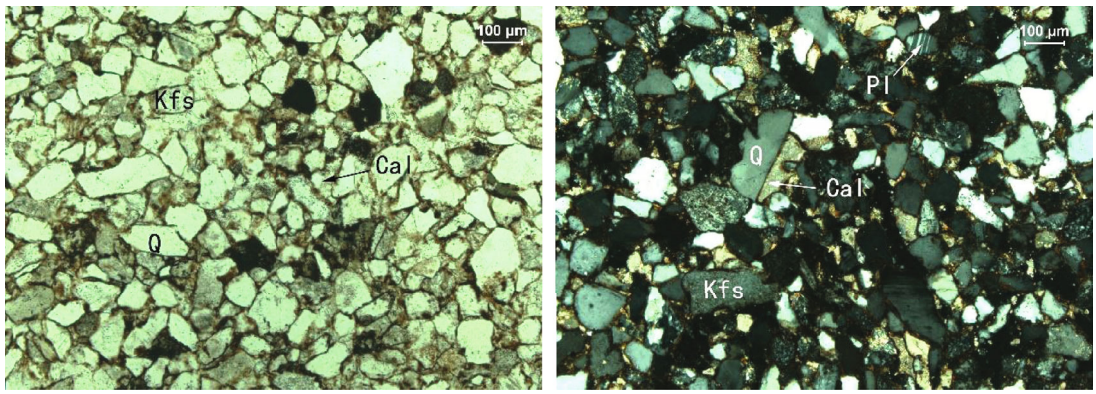

Figure 1: Optical microscopy analysis of the sandstone.

become stable. It is universally accepted that the mechanical behavior of rock materials tested under wet conditions is more sensitive to low temperature than that tested under dry condition [9]. For the wet rock under subzero temperatures, it can be considered as a water-ice-rock mixture [13]. Prior studies indicate that the mechanical response of frozen rock is very complicated, and the mechanical characteristics are controlled by the coupled effects of water weakening and ice enhancing. To be specific, the presence of water has weakening effects on rock strength and stiffness [14–18], whereas the ice can resist the rock deformation to enhance the rock integrity [19–21].

The abovementioned works mainly focus on the mechanical properties of rock under subzero temperatures tested in quasistatic loading conditions, in which the strain rate of rock specimen is very low around the magnitude of 10^{-4} s^{-1}. However, in some particular engineering projects constructed in cold regions, rock masses inevitably suffer from low-temperature weathering and dynamic disturbances concurrently [22]. The dynamic disturbances probably come from mining, drilling tunneling, or seismic activities [14, 15, 23–25]. As evidenced by previous studies [26, 27], the mechanical behavior of rocks under dynamic loadings is remarkably different from that under static ones [28]. Hence, it is necessary to study the dynamic mechanical properties of rocks at extremely low temperature.

The objective of the present study is to investigate the effects of low temperature on the dynamic mechanical behavior of rock. Series of high strain rate tests were conducted on dry and water-saturated sandstone specimens under room temperature and -60°C by using a split Hopkinson pressure bar apparatus. Quasistatic compressive tests were also performed for comparison. The effects of temperature and strain rate on dynamic strength, Young's modulus, failure strain, and energy dissipation were obtained. The water-weakening and ice-enhancing mechanisms for mechanical properties of water-saturated sandstone specimens at -60°C were discussed.

Table 1: Mineral composition of sandstone specimen.

Mineral composition	Content (%)
Quartz	46
Potash feldspar	18
Calcite	18
Plagioclase	8
Hematite	5
Chlorite	2
Sericite	2

Figure 2: MTS-322 used for quasistatic tests.

2. Experimental Material and Methodology

2.1. Description of Rock Material. The rock material used in this study is a sandstone collected from the southwest area of Sichuan province, China. Figure 1 presents microscopic images of the sandstone using optical microscopy. The sandstone is fine-grained, and its cementation type is pore cementation. The mineral compositions of this sandstone

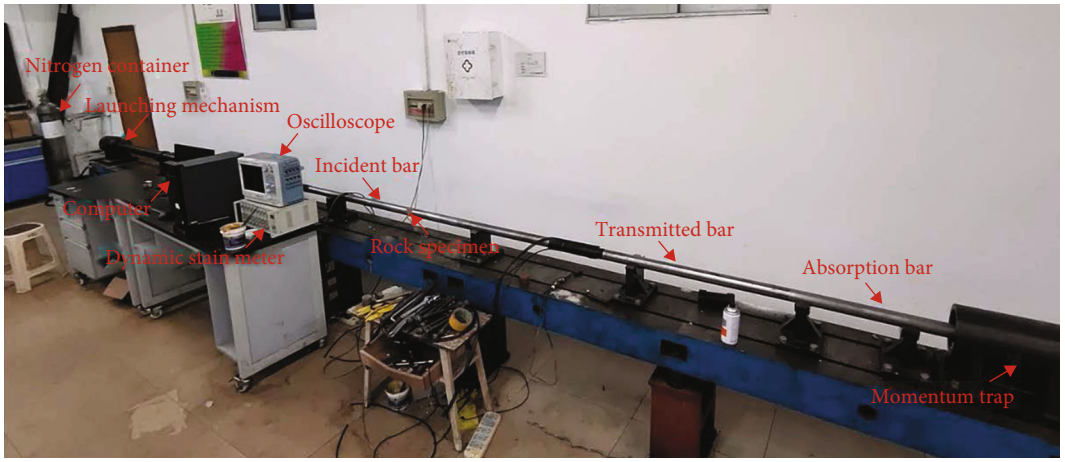

Figure 3: Photographic view of SHPB setup.

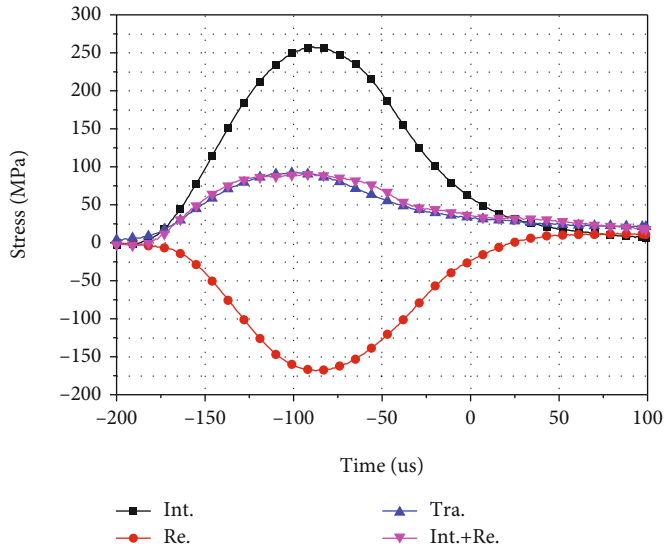

Figure 4: Dynamic force equilibrium.

and corresponding percentage were determined by the X-ray diffraction (XRD) technique. As listed in Table 1, the sandstone consists mainly of five minerals, including quartz (46%), potash feldspar (18%), calcite (18%), plagioclase (8%), and hematite (5%). The chlorite and sericite contents are less than 2% by weight. Crucial physical parameters of the sandstone were also measured as density of 2410 kg/m^3, P-wave velocity of 3499 m/s, and water absorption of 3.37%.

2.2. Specimen Preparation. All specimens were manufactured in accordance with standards of the International Society for Rock Mechanics and Rock Engineering (ISRM) [29, 30]. To minimize the variation in properties across the specimens and reduce the dispersion of tested data, all cores in 50 mm diameter were first drilled from the same rock in the same direction. After which, rock cores were cut into the specified lengths. For quasistatic tests, the aspect ratio of specimens is about 2.0 while that for dynamic tests is 1.0. Then, the ends of all specimens were polished with a grinder to make the surface roughness less than 0.05 mm, and the end face was

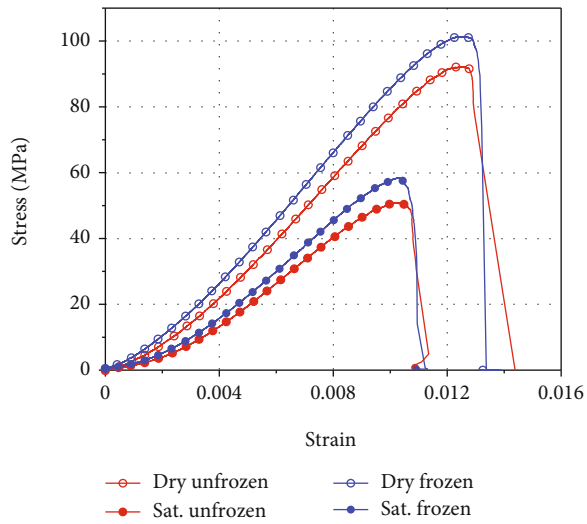

Figure 5: Stress-strain curves of dry and water-saturated specimens tested under uniaxial compression.

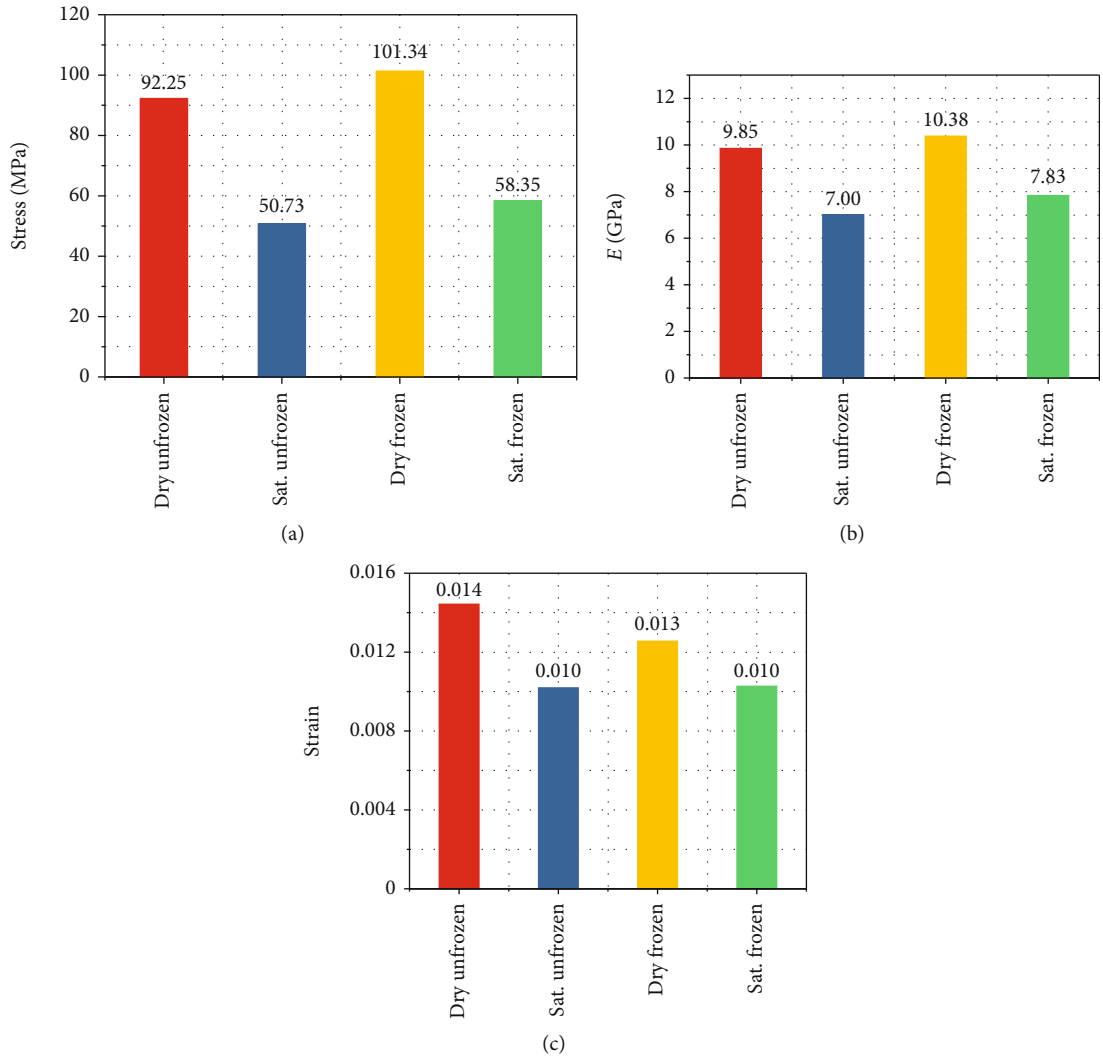

Figure 6: The (a) UCS, (b) E, and (c) failure strain values of specimens under uniaxial compression.

vertical to the axis of the specimen with a deviation less than 0.25°.

All specimens were placed in an oven set at the 105°C constant temperature for more than 48 h to remove the moisture in specimens. After that, they were taken out and placed in laboratory for air-cooling. Then, half of them were submerged in distilled water for at least 48 h for free soaking such that specimens can reach a water-saturation state [16, 31]. To prepare frozen specimens, half specimens were chosen from each dry and saturated set of specimens. They were put in a refrigerator at a constant temperature of -60°C for more than 48 h.

2.3. Experimental Apparatus

2.3.1. Quasistatic Test. Quasistatic uniaxial compression tests were conducted on an electrohydraulic servo material testing machine (MTS-322) housed in Advance Research Center of Central South University, China, as shown in Figure 2. The maximum vertical load of the device is up to 500 kN, and the overall stiffness is 1370 kN/mm. The machine can successfully reproduce the failure process of rock under low strain rates and has been extensively used in the testing of rock mechanics [32–34]. In this study, the loading speed was maintained at 0.24 mm/min, i.e., the strain rate of specimens in quasistatic tests was 4×10^{-5} s^{-1}.

2.3.2. Split Hopkinson Pressure Bar System. A split Hopkinson pressure bar (SHPB) device is used to conduct dynamic compressive tests [35]. It can realize the dynamic testing on rock materials within the range of strain rate from 10^0 to 10^2 s^{-1} [15, 36]. As shown in Figure 3, the SHPB system consists of a gas gun, a striker, three 50 mm diameter bars (called incident bar, transmitted bar, and absorption bar), and a momentum trap. The cone-shaped striker invented by Li et al. [37, 38] is applied to generate a half-sine wave for achieving stress equilibrium and avoiding premature failure of rock material. All of the bars and striker are made of high-strength 40 chromium alloy with a density of 7821 kg/m^3, an elastic modulus of 233 GPa, and a longitudinal wave velocity is 5462 m/s. In tests, the specimen is sandwiched between the incident and transmitted bars. The

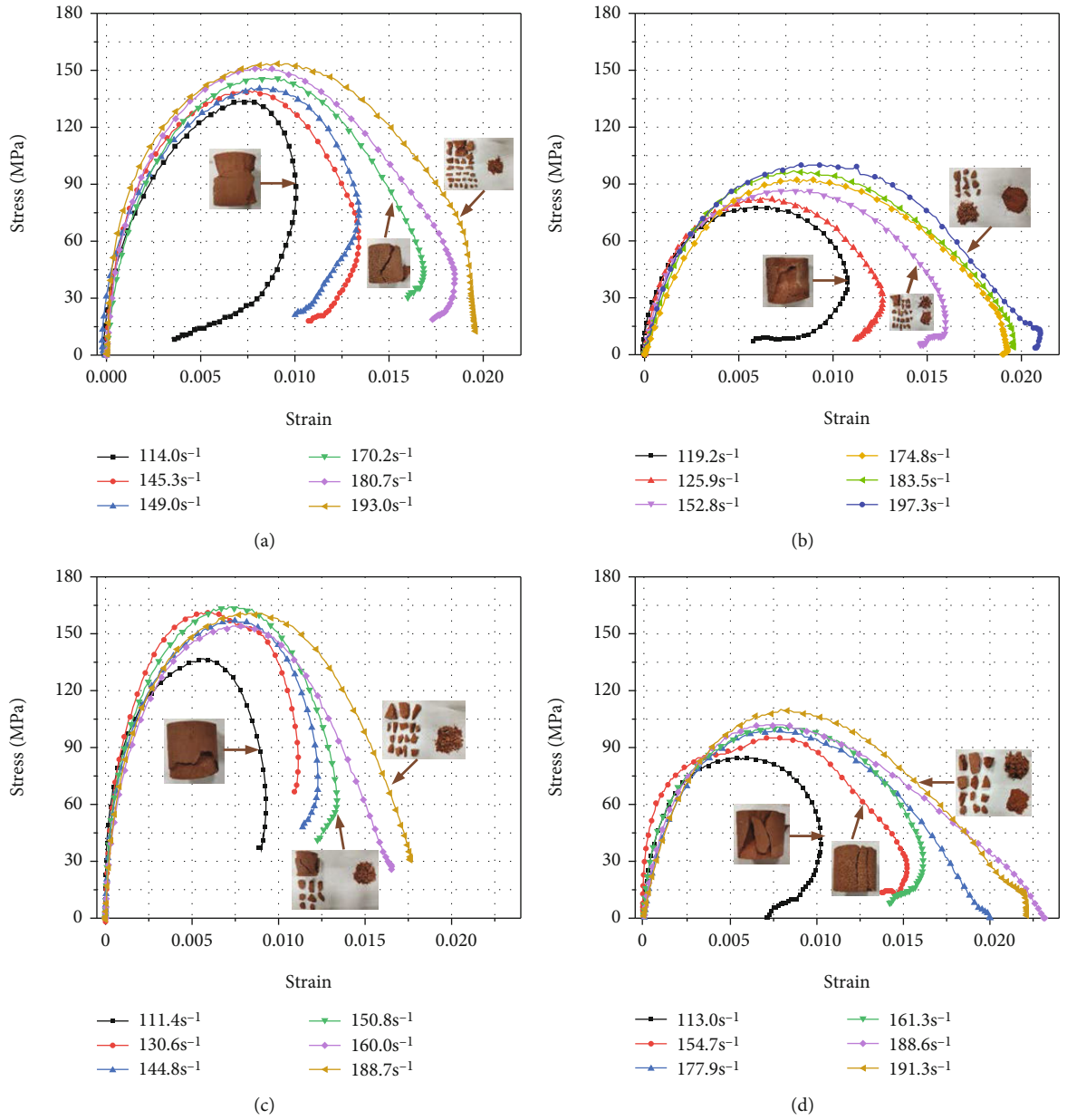

Figure 7: Dynamic stress-strain curves of (a) dry unfrozen, (b) saturated unfrozen, (c) dry frozen, and (d) saturated frozen specimens under different strain rates.

interfaces are smeared with sufficient lubricant to eliminate the end friction effect [27, 39, 40].

The cone-shaped striker is shot from the gas gun with a high velocity and impacts the end of the incident bar. Meanwhile, a slow-rising half-sine wave is produced and propagates along the incident bar (called incident wave). When the wave arrives in the interface between the incident bar and the specimen, a portion of it will be reflected to the incident bar (called reflected wave) due to the difference in wave impedance, and the other portion will pass through the specimen and transmitted into the transmitted bar (called transmitted wave). The three waves are monitored by strain gages glued on the middle of the incident and transmitted bars and then recorded by a digital oscilloscope.

2.4. Data Processing

2.4.1. Dynamic Stress Equilibrium. In SHPB tests, one of the prerequisites for test validity is the specimen reaching the stress equilibrium before failure. Herein, the dynamic stress equilibrium of the specimen is strictly examined by comparing the dynamic stress on both sides of the specimen. Figure 4 depicts the stress history on both sides of the specimen in a typical dynamic SHPB test. The time zeros of the incident wave and reflected wave are moved to the specimen/incident bar interface, and the time zero of the transmitted wave is shift to the specimen/transmitted bar interface. From Figure 4, the sum of the incident and the reflected stresses is almost equal to the value of transmitted stress during the

Table 2: Parameters and test results of the specimens in SHPB tests.

SN	Length (mm)	Diameter (mm)	P-wave (m/s)	Mass (g)	Strain rate (s^{-1})	UCS_d (MPa)	E_d (GPa)
DU-1	50.21	49.18	3536.15	230.07	114.01	133.54	13.56
DU-2	50.25	49.15	3513.99	230.98	145.28	139.16	13.32
DU-3	50.27	49.16	3490.74	229.54	149.05	140.75	13.62
DU-4	50.20	49.14	3510.26	228.76	170.18	145.68	13.65
DU-5	50.19	49.14	3509.56	229.83	180.68	151.18	13.93
DU-6	50.07	49.17	3525.82	228.56	193.00	153.43	14.02
SU-1	50.21	49.22	3511.19	229.52	119.20	78.19	9.71
SU-2	50.21	49.17	3487.04	229.55	125.90	82.66	9.98
SU-3	50.27	49.21	3490.97	229.80	152.80	86.57	10.23
SU-4	50.29	49.18	3541.55	230.51	174.80	92.26	9.95
SU-5	50.27	49.12	3442.92	231.11	183.50	96.98	10.56
SU-6	50.14	49.15	3434.47	229.03	197.30	100.01	10.79
DF-1	50.31	49.17	3493.75	230.88	111.39	136.76	15.62
DF-2	50.23	49.18	3613.43	229.90	130.57	161.07	16.30
DF-3	50.28	49.18	3516.32	229.36	144.82	156.86	16.00
DF-4	50.23	49.14	3587.86	231.13	150.76	164.07	16.02
DF-5	50.29	49.19	3492.13	231.08	159.97	154.04	15.70
DF-6	50.29	49.26	3468.51	229.98	188.68	160.69	16.33
SF-1	50.27	49.27	3490.97	228.97	113.03	84.72	10.26
SF-2	50.36	49.21	3571.63	229.64	154.69	95.02	9.98
SF-3	50.24	49.18	3513.05	230.14	177.85	98.98	11.09
SF-4	50.21	49.17	3438.81	229.04	161.33	100.75	10.78
SF-5	50.22	49.14	3416.33	229.28	188.63	102.04	11.05
SF-6	50.25	49.16	3514.22	230.05	191.26	110.10	11.22

Note: DU: dry unfrozen specimen; SU: saturated unfrozen specimen; DF: dry frozen specimen; SF: saturated frozen specimen; UCS_d: dynamic uniaxial compressive strength; E_d: dynamic elastic modulus.

whole loading process. In this case, the axial inertial effect can be ignored due to the fact that there is no overall force difference in the specimen to cause inertial force. Therefore, the SHPB test is valid.

2.4.2. Determination of Stress, Strain, and Strain Rate. According to the theory of one-dimensional wave, the histories of stress, strain rate, and strain in the specimen subjected to dynamic loading can be calculated by the three-wave method as [29, 41].

$$\begin{cases} \sigma_d(t) = \dfrac{A_b E_b}{2A_s}[\varepsilon_i(t) + \varepsilon_r(t) + \varepsilon_t(t)], \\ \varepsilon(t) = \dfrac{C_b}{L_s}\displaystyle\int_0^t [\varepsilon_i(t) - \varepsilon_r(t) - \varepsilon_t(t)]dt, \\ \dot{\varepsilon}(t) = \dfrac{C_b}{L_s}[\varepsilon_i(t) - \varepsilon_r(t) - \varepsilon_t(t)], \end{cases} \tag{1}$$

where σ_d, ε, and $\dot{\varepsilon}$ are the dynamic compressive stress, strain, and strain rate of the specimen, respectively; A_b, E_b, and C_b are the cross-sectional area, elastic modulus, and P-wave velocity of elastic bars; A_s and L_s are the cross-sectional area and length of the specimen; and ε_i, ε_r, and ε_t are incident, reflected, and transmitted wave signals. The strain rates of specimens are controlled by the impact velocity of the striker, which can be adjusted to the actuating gas pressure in the gas gun.

3. Experimental Results

3.1. Quasistatic Mechanical Behavior of Dry and Water-Saturated Sandstone. Figure 5 presents the typical stress-strain curves of dry and water-saturated specimens tested under room temperature and -60°C. Apparent changes in the shape of the curve can be observed between dry and saturated specimens at the same temperature but not found between frozen and unfrozen specimens in the same water condition. This means that in quasistatic condition, the dominant factor controlling the rock properties is water rather than temperature. Average values of uniaxial compressive strength (UCS), Young's modulus (E), and failure strain of specimens are depicted in Figure 6. As shown in Figure 6(a), it can be clearly seen that the presence of water significantly weakens the UCS of sandstone specimens. At room temperature and -60°C, the water-induced loss percentage in UCS is 45.0% and 42.4%, respectively. However, for dry and water-saturated specimens, the UCS tested at -60°C is 8.97%, 13.1% higher than that tested at room temperature, respectively. The possible reason is that the frozen pore water can enhance the rock strength to some extent.

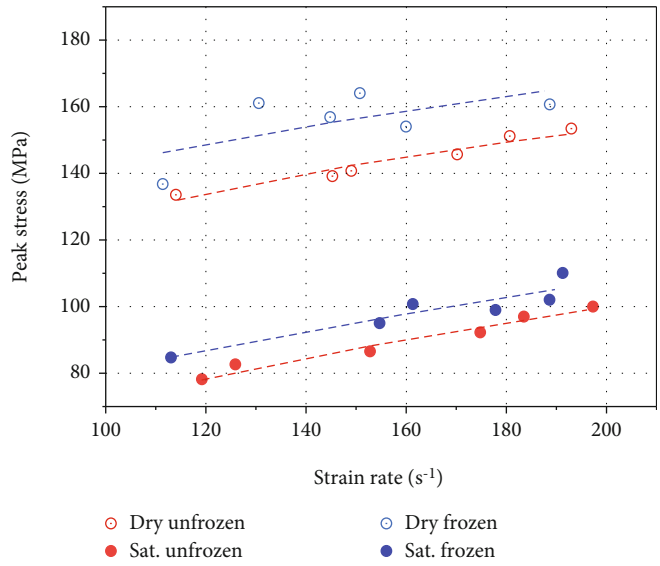

Figure 8: Variations in UCS_d against strain rate under four conditions.

From Figures 6(b) and 6(c), Young's modulus and failure strain follow a similar changing pattern as for UCS. This indicates that the water plays dual effects at subzero temperature.

3.2. Dynamic Mechanical Behavior of Dry and Water-Saturated Sandstone

3.2.1. Dynamic Stress-Strain Curves of Dry and Water-Saturated Specimens under Room Temperature and -60°C. Figure 7 presents the dynamic stress-strain curves of dry and saturated specimens tested at room temperature and -60°C. In each case, stress-strain curves obtained from six different strain rates are plotted. Before peak stress, the dynamic stress-strain curves show a similar pattern. However, the postpeak stress-strain curves are very different, indicating different final pattern. The apparent rebounding of postpeak curve means that the specimen is unbroken when subjected to dynamic loading, such as in Figure 7(a) curve with a strain rate of 114 s^{-1}. This is due to the fact that the incident energy is not enough to break the rock specimen [14]. The other curves in postpeak regime show strain softening, i.e., the stress decreases as the strain increases, leaving a large residual strain, such as Figure 7(a) curve with a strain rate of 193 s^{-1}. This indicates the specimen is fractured and loses its cohesion.

3.2.2. Dynamic Strength of Dry and Water-Saturated Specimens under Room Temperature and -60°C. According to dynamic stress-strain curves, dynamic parameters of each specimen are obtained as listed in Table 2.

The variations of peak stress versus strain rate for dry and water-saturated specimens under room temperature and -60°C are plotted in Figure 8. It can be seen that regardless of temperature and water conditions, the peak stress increases with the rise of the strain rate. Both low temperature and water saturation play crucial factors in controlling the peak stress of the specimen. When tested at the same temperature, the peak stress of water-saturated specimen is much lower than that of dry ones at similar strain rates. This is caused by water-weakening effects.

Table 3: Fitting parameters of the relationship between dynamic strength and strain rate.

	Fitting relationship
Dry unfrozen	$UCS_d = 35.6140\dot{\varepsilon}^{0.276}$
Saturated unfrozen	$UCS_d = 8.8165\dot{\varepsilon}^{0.458}$
Dry frozen	$UCS_d = 49.797\dot{\varepsilon}^{0.229}$
Saturated frozen	$UCS_d = 11.388\dot{\varepsilon}^{0.423}$

The strength changes of these four types of rocks can be fitted with the exponential fitting relationship as follows:

$$UCS_d = a * \dot{\varepsilon}^b, \quad (2)$$

where a and b are the fitting parameters, b is the regression coefficient. The larger the absolute value of b, the higher the growth rate of the UCS_d. The specific fitting relationship is shown in Table 3.

A dynamic increasing factor (η), defined as the ratio of dynamic strength to quasi-static one ($\eta = \sigma_d/\sigma_s$), is introduced to quantify the strain rate effect on rock strength. From Figure 9, it can be seen that η apparently increases as the strain rate rises. Interestingly, η under different moisture and temperature conditions is very distinct. At the same strain rate, the saturated-unfrozen specimen has the largest value of η, followed by saturated frozen, dry frozen, and dry unfrozen specimens in descending order. This indicates that the presence of water plays a more important role in controlling the rate dependence of rock strength compared to low temperature.

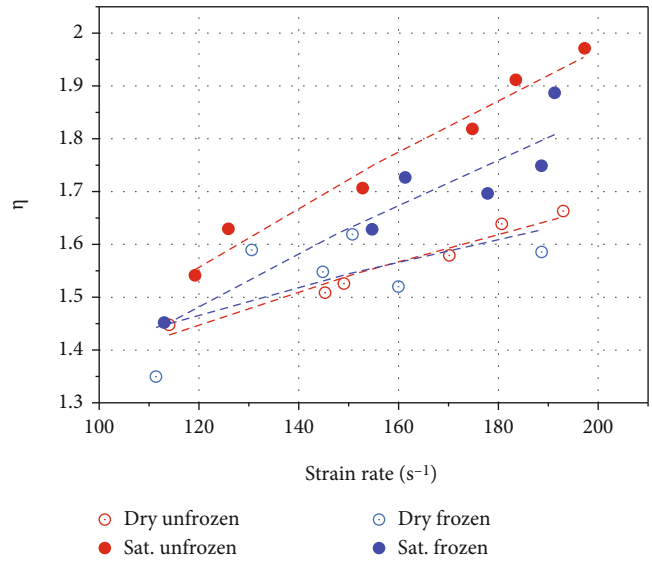

Figure 9: Variations of dynamic increasing factor against strain rate.

3.2.3. Changes in E_d of Dry and Saturated Specimens at Room and Subzero Temperatures. Figure 10 shows the variation in the dynamic elastic modulus of sandstone under different conditions versus strain rate. Unlike the dynamic strength, the dynamic elastic modulus nearly keeps constant in the testing range of strain rate for each condition. This implies that the dynamic elastic modulus is not sensitive to strain rate, which agrees with prior test results on other rock-like materials, such as concrete [41], sandstone [14], marble [42], limestone [43], and granite [44]. This is possibly due to the fact that the initial elastic modulus under dynamic loads is not affected by strain rate since no significant microcrack creates during the initial loading stage, as shown in Figure 7.

From Figure 10, it can be also seen that, under each condition, the average dynamic elastic modulus is greater than the quasistatic value (see Figure 6(b)) probably due to the inertial effect. Moreover, no matter on frozen or unfrozen condition, the water-saturated specimen has the lower dynamic modulus than the dry one. The observation is contrary to many previous studies [14, 41], in which the dynamic elastic modulus will increase when the rock becomes water-saturated.

3.2.4. The Energy Absorption of Dry and Saturated Specimens at Room and Subzero Temperatures. To characterize the prepeak (e_f) and total absorbed (e_t) energy, the shadow areas under stress-strain curves before peak stress and during the whole loading process are calculated [45], as shown in Figure 11.

Figure 12 gives the results of energy absorbed in dynamic tests. It can be found that, for each condition, both of prepeak and total energy absorption rise with the increasing strain rate. There is no obvious difference in energy absorption between dry-frozen and dry-unfrozen specimens exposed to the same strain rate also between saturated-frozen and saturated-unfrozen specimens. In addition, regardless of temperature, dry specimens consume much more energy than saturated ones. These phenomena indicate that the water significantly lowers the energy needed to break the rock but the tested temperature has negligible effect.

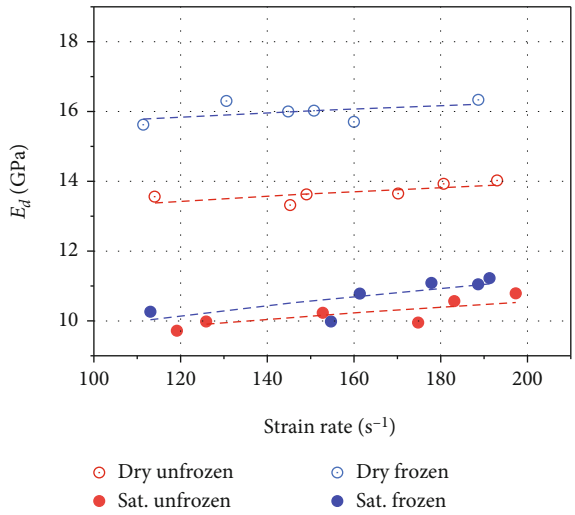

Figure 10: Variations in E_d against strain rate.

4. Discussion

4.1. Effects of Water Saturation on Rock Strength

4.1.1. Water-Weakening Effects. At room temperature, water weakens rock strength in quasistatic tests [18]. Prior researchers proposed several mechanisms to reveal this phenomenon, such as (1) the reduction of fracture energy [17], (2) quartz hydrolysis [46–48], (3) friction reduction, and [31, 49] (4) chemical and physical deterioration [50, 51].

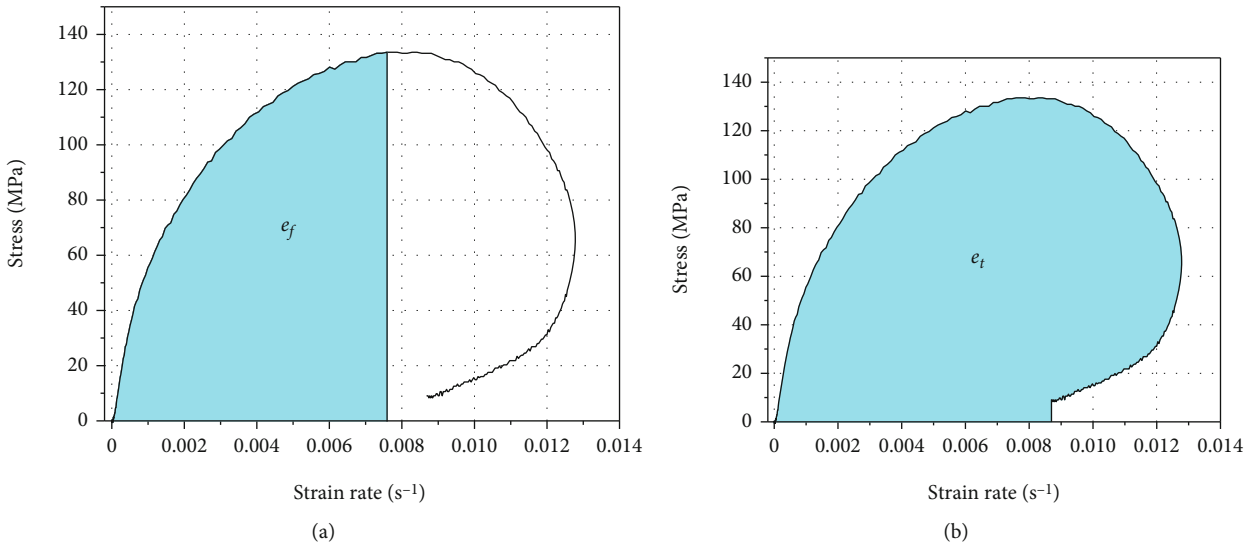

Figure 11: Calculation of energy absorption per unit volume: (a) absorption energy before peak stress and (b) total absorption energy.

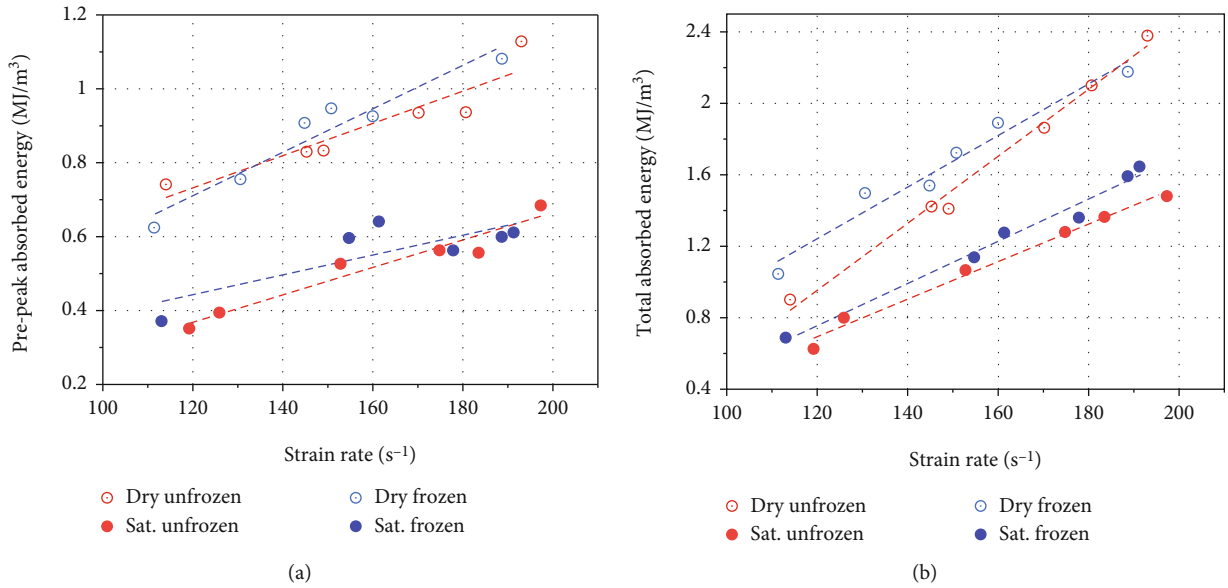

Figure 12: Variations of (a) e_f and (b) e_t versus strain rate.

For the sandstone, the friction reduction can be ignored because of the absence of minerals. Coupled effects of fracture energy reduction, quartz hydrolysis, and chemical and physical deterioration result in the loss of strength. Possible chemical reactions are listed in Table 4.

4.1.2. Water-Enhancing Effects. When the rock specimen is subjected to dynamic loading, free water in rock defects will hinder crack initiation and propagation through the following aspects: (1) the increase of inertia [15], (2) the reduction of local damage [52], (3) meniscus effect [53, 54], and (4) viscous effects [53]. These will increase the dynamic strength of rock to some extent and enhance the rate dependence of rock strength.

4.2. Effects of Subzero Temperature on Rock Strength

4.2.1. Subzero Temperature Enhancing Effects. Under subzero temperature condition, water in rock will be frozen. As a solid, ice can support external force with rock skeleton [6]. Also, ice can connect and tighten neighbouring grains and particles like binding agent [20]. In addition, subzero temperature makes the matrix group of mineral particles more compact and enhances the ability to resist deformation [20]. These are beneficial for rock strength.

4.2.2. Subzero Temperature Weakening Effects. When rock is completely saturated, water is filled with all connected pores. When the rock is exposed to subzero temperature, the dilation of frozen water will exert pore pressure to cause pore damage [20].

Table 4: Possible chemical reactions between water and minerals during water immersion.

Mineral	Chemical reaction formula
Quartz (46%)	$SiO_2 + Al_2O_3 + H_2O \longrightarrow \left[mSiO_2g2H_2OgnSiO_3^{2-}\right]^{x-} + \left[mAl(OH)_3gnAl(OH)_2^{+}\right]^{x+}$
Potash feldspar (18%)	$K[AlSi_3O_8] + H^+ + OH^- \longrightarrow Al_4Si_4O_{10}(OH)_8 + H_4SiO_4 + K^+$
Calcite (18%)	$CaCO_3 + CO_2 + H_2O \longrightarrow Ca(HCO_3)_2$
Plagioclase (8%)	$CaAl_2Si_2O_8 + CO_2 + H_2O \longrightarrow CaCO_3 + Al_2Si_2O_5\,(OH)_4$

4.3. Coupled Effects of Water Saturation and Subzero Temperature on the Compressive Strength of Sandstone. Test results show that the sandstone under dry frozen condition has the maximum UCS, followed by that under dry unfrozen, saturated frozen, and saturated unfrozen conditions. For the dry frozen specimen, the subzero temperature enhancing effects dominates the increase of UCS. While for the saturated unfrozen specimen, water-weakening effects are responsible for the dramatic drop in UCS. When the saturated specimen is exposed to subzero temperature, the affecting mechanisms of rock strength are very complicated. On the one hand, water-weakening effects and subzero temperature weakening effects deteriorate rock skeleton and make serious damage in rock. On the other hand, the concretion and connection effects of ice can strengthen the rock. For the tested sandstone, the water-weakening effects are very significant. The subzero temperature enhancing effects are not enough to fully compensate for the UCS loss induced by water weakening. This leads to that the UCS of the saturated frozen specimen is evidently lower than that of the dry specimen but slightly greater than that of saturated unfrozen one.

In fact, when subjected to dynamic loading, the enhancing effects of free water work to rise the UCS. The rate dependence of UCS is primarily controlled by the content of liquid water in rock. Water will freeze under subzero temperature such that the content of liquid water decreases. Therefore, the saturated unfrozen specimen holds the maximum rate dependence of UCS while the UCS rate dependence of saturated frozen specimen, dry unfrozen specimen, and dry frozen specimen decreases in the cited order.

5. Conclusions

In this paper, quasistatic and dynamic compressive tests were performed on dry and water-saturated sandstone specimens under room and -60°C temperatures. The mechanical properties of specimens under different conditions were obtained. The coupled effects of water and low temperature on rock behavior were revealed. The following conclusions can be drawn:

(1) At room temperature, in both quasistatic and dynamic loading condition, when the rock specimen becomes water-saturated from dry condition, its strength and elastic modulus are significantly decreased

(2) The subzero temperature enhances the compressive strength and elastic modulus of dry and water-saturated specimens, such that these mechanical parameters at subzero temperature are notably greater than that at room temperature. However, due to the water-weakening effects, the strength and elastic modulus of the saturated-frozen specimen are still lower than that of the dry-frozen and dry-unfrozen specimens

(3) The compressive strength of sandstone is rate-dependent. The saturated unfrozen specimen has the highest rate dependence of strength, followed by the saturated frozen, dry unfrozen, and dry frozen specimens in degressive order. Contrarily, the elastic modulus of sandstone seems to be not sensitive to strain rate

Data Availability

The data used to support the findings of this study are available from the corresponding authors upon request.

Conflicts of Interest

The authors declare that there is no conflict of interest regarding the publication of this paper.

Acknowledgments

This work was supported by the National Natural Science Foundation of China (41772313), Hunan Science and Technology Planning Project (No. 2019RS3001), and the Graduated Students' Research and Innovation Fund Project of Central South University (2020zzts710). The authors are very grateful for the financial contributions and convey their appreciation to the organizations for supporting this basic research.

References

[1] Z. Song, Y. Wang, H. Konietzky, and X. Cai, "Mechanical behavior of marble exposed to freeze-thaw-fatigue loading," *International Journal of Rock Mechanics and Mining Sciences*, vol. 138, article 104648, 2021.

[2] H. Zhong-Wei, W. Jiang-Wei, L. I. Gen-Sheng, and C. Cheng-Zheng, "An experimental study of tensile and compressive strength of rocks under cryogenic nitrogen freezing," *Rock and Soil Mechanics*, vol. 37, no. 3, pp. 694–700,834, 2016.

[3] R. Yang, S. Fang, W. Li, Y. Yang, and Z. Yue, "Experimental study on the dynamic properties of three types of rock at

negative temperature," *Geotechnical and Geological Engineering*, vol. 37, no. 1, pp. 455–464, 2018.

[4] W. Chen, X. Tan, H. Yu, K. Yuan, and S. Li, "Advance and review on thermo-hydro-mechanical characteristics of rock mass under condition of low temperature and freeze-thaw cycles," *Chinese Journal of Rock Mechanics and Engineering*, vol. 30, no. 7, pp. 1318–1336, 2011.

[5] H. Jia, F. Zi, G. Yang et al., "Influence of pore water (ice) content on the strength and deformability of frozen argillaceous siltstone," *Rock Mechanics and Rock Engineering*, vol. 53, no. 2, pp. 967–974, 2020.

[6] J. Kodama, T. Goto, Y. Fujii, and P. Hagan, "The effects of water content, temperature and loading rate on strength and failure process of frozen rocks," *International Journal of Rock Mechanics and Mining Sciences*, vol. 62, pp. 1–13, 2013.

[7] E. M. Winkler, "Frost damage to stone and concrete: geological considerations," *Engineering Geology*, vol. 2, no. 5, pp. 315–323, 1968.

[8] Y. Inada and K. Yokata, "Some studies of low temperature rock strength," *International Journal of Rock Mechanics and Mining Sciences & Geomechanics Abstracts*, vol. 21, no. 3, pp. 145–153, 1984.

[9] K. Aoki, K. Hibiya, and T. Yoshida, "Storage of refrigerated liquefied gases in rock caverns: characteristics of rock under very low temperatures," *Tunnelling and Underground Space Technology*, vol. 4, no. 5, pp. 319–325, 1990.

[10] T. Yamabe and K. M. Neaupane, "Determination of some thermo-mechanical properties of Sirahama sandstone under subzero temperature condition," *International Journal of Rock Mechanics and Mining Sciences*, vol. 38, no. 7, pp. 1029–1034, 2001.

[11] R. D. Dwivedi, A. K. Soni, R. K. Goel, and A. K. Dube, "Fracture toughness of rocks under sub-zero temperature conditions," *International Journal of Rock Mechanics and Mining Sciences*, vol. 37, no. 8, pp. 1267–1275, 2000.

[12] T. Mingming, W. Zhiyin, S. Yili, and B. Jinhong, "Experimental study of mechanical properties of granite under low temperature," *Chinese Journal of Rock Mechanics and Engineering*, vol. 29, no. 4, pp. 787–794, 2010.

[13] L. Weng, Z. Wu, A. Taheri, Q. Liu, and H. Lu, "Deterioration of dynamic mechanical properties of granite due to freeze-thaw weathering: considering the effects of moisture conditions," *Cold Regions Science and Technology*, vol. 176, article 103092, 2020.

[14] X. Cai, Z. Zhou, H. Zang, and Z. Song, "Water saturation effects on dynamic behavior and microstructure damage of sandstone: phenomena and mechanisms," *Engineering Geology*, vol. 276, article 105760, 2020.

[15] Z. Zhou, X. Cai, D. Ma et al., "Water saturation effects on dynamic fracture behavior of sandstone," *International Journal of Rock Mechanics and Mining Sciences*, vol. 114, pp. 46–61, 2019.

[16] X. Cai, Z. Zhou, L. Tan, H. Zang, and Z. Song, "Water saturation effects on thermal infrared radiation features of rock materials during deformation and fracturing," *Rock Mechanics and Rock Engineering*, vol. 53, no. 11, pp. 4839–4856, 2020.

[17] X. Cai, Z. Zhou, and X. Du, "Water-induced variations in dynamic behavior and failure characteristics of sandstone subjected to simulated geo-stress," *International Journal of Rock Mechanics and Mining Sciences*, vol. 130, article 104339, 2020.

[18] D. Ma, H. Duan, W. Liu, X. Ma, and M. Tao, "Water–sediment two-phase flow inrush Hazard in rock fractures of overburden strata during coal mining," *Mine Water and the Environment*, vol. 39, no. 2, pp. 308–319, 2020.

[19] T. C. Chen, M. R. Yeung, and N. Mori, "Effect of water saturation on deterioration of welded tuff due to freeze-thaw action," *Cold Regions Science and Technology*, vol. 38, no. 2-3, pp. 127–136, 2004.

[20] L. Weng, Z. Wu, and Q. Liu, "Dynamic mechanical properties of dry and water-saturated siltstones under sub-zero temperatures," *Rock Mechanics and Rock Engineering*, vol. 53, no. 10, pp. 4381–4401, 2020.

[21] S. Huang, Q. Liu, A. Cheng, Y. Liu, and G. Liu, "A fully coupled thermo-hydro-mechanical model including the determination of coupling parameters for freezing rock," *International Journal of Rock Mechanics and Mining Sciences*, vol. 103, pp. 205–214, 2018.

[22] L. Weng, Z. Wu, Q. Liu, and Z. Wang, "Energy dissipation and dynamic fragmentation of dry and water-saturated siltstones under sub-zero temperatures," *Engineering Fracture Mechanics*, vol. 220, article 106659, 2019.

[23] S. Wang, X. Li, K. Du, and S. Wang, "Experimental investigation of hard rock fragmentation using a conical pick on true triaxial test apparatus," *Tunnelling and Underground Space Technology*, vol. 79, pp. 210–223, 2018.

[24] Z. Song, T. Frühwirt, and H. Konietzky, "Inhomogeneous mechanical behaviour of concrete subjected to monotonic and cyclic loading," *International Journal of Fatigue*, vol. 132, article 105383, 2019.

[25] Y. Wang, W. K. Feng, R. L. Hu, and C. H. Li, "Fracture evolution and energy characteristics during marble failure under triaxial fatigue cyclic and confining pressure unloading (FC-CPU) conditions," *Rock Mechanics and Rock Engineering*, vol. 54, no. 2, pp. 799–818, 2021.

[26] X. Cai, Z. Zhou, L. Tan, H. Zang, and Z. Song, "Fracture behavior and damage mechanisms of sandstone subjected to wetting- drying cycles," *Engineering Fracture Mechanics*, vol. 234, article 107109, 2020.

[27] Q. B. Zhang and J. Zhao, "A review of dynamic experimental techniques and mechanical behaviour of rock materials," *Rock Mechanics and Rock Engineering*, vol. 47, no. 4, pp. 1411–1478, 2014.

[28] Y. Wang, C. H. Li, and J. Q. Han, "On the effect of stress amplitude on fracture and energy evolution of pre- flawed granite under uniaxial increasing-amplitude fatigue loads," *Engineering Fracture Mechanics*, vol. 240, article 107366, 2020.

[29] Y. X. Zhou, K. Xia, X. B. Li et al., "Suggested methods for determining the dynamic strength parameters and mode-I fracture toughness of rock materials," *International Journal of Rock Mechanics and Mining Sciences*, vol. 49, pp. 105–112, 2012.

[30] Z. T. Bieniawski and M. J. Bernede, "Suggested methods for determining the uniaxial compressive strength and deformability of rock materials," *International Journal of Rock Mechanics & Mining Sciences & Geomechanics Abstracts*, vol. 16, no. 2, pp. 138–140, 1979.

[31] X. Cai, Z. Zhou, K. Liu, X. Du, and H. Zang, "Water-weakening effects on the mechanical behavior of different rock types: phenomena and mechanisms," *Applied Sciences*, vol. 9, no. 20, article 4450, 2019.

[32] K. Du, X. Li, M. Tao, and S. Wang, "Experimental study on acoustic emission (AE) characteristics and crack classification

during rock fracture in several basic lab tests," *International Journal of Rock Mechanics and Mining Sciences*, vol. 133, article 104411, 2020.

[33] K. Du, R. Su, M. Tao, C. Yang, A. Momeni, and S. Wang, "Specimen shape and cross-section effects on the mechanical properties of rocks under uniaxial compressive stress," *Bulletin of Engineering Geology and the Environment*, vol. 78, no. 8, pp. 6061–6074, 2019.

[34] Z. Zhou, X. Cai, W. Cao, X. Li, and C. Xiong, "Influence of water content on mechanical properties of rock in both saturation and drying processes," *Rock Mechanics and Rock Engineering*, vol. 49, no. 8, pp. 3009–3025, 2016.

[35] Q. Wu, X. Li, L. Weng, Q. Li, Y. Zhu, and R. Luo, "Experimental investigation of the dynamic response of prestressed rockbolt by using an SHPB-based rockbolt test system," *Tunnelling and Underground Space Technology*, vol. 93, article 103088, 2019.

[36] X. Li, *Rock Dynamics: Fundamentals and Applications*, Science Press, Beijing, 2014.

[37] X. Li, Z. Zhou, T. Lok, L. Hong, and T. Yin, "Innovative testing technique of rock subjected to coupled static and dynamic loads," *International Journal of Rock Mechanics and Mining Sciences*, vol. 45, no. 5, pp. 739–748, 2008.

[38] Z. Zhou, X. Li, Z. Ye, and K. Liu, "Obtaining constitutive relationship for rate-dependent rock in SHPB tests," *Rock Mechanics and Rock Engineering*, vol. 43, no. 6, pp. 697–706, 2010.

[39] Z. Zhou, X. Cai, X. Li, W. Cao, and X. Du, "Dynamic response and energy evolution of sandstone under coupled static–dynamic compression: insights from experimental study into deep rock engineering applications," *Rock Mechanics and Rock Engineering*, vol. 53, no. 3, pp. 1305–1331, 2020.

[40] Q. Wu, L. Chen, B. Shen, B. Dlamini, S. Li, and Y. Zhu, "Experimental investigation on rockbolt performance under the tension load," *Rock Mechanics and Rock Engineering*, vol. 52, no. 11, pp. 4605–4618, 2019.

[41] W. Ren, J. Xu, J. Liu, and H. Su, "Dynamic mechanical properties of geopolymer concrete after water immersion," *Ceramics International*, vol. 41, no. 9, pp. 11852–11860, 2015.

[42] M. Doan and A. Billi, "High strain rate damage of Carrara marble," *Geophysical Research Letters*, vol. 38, no. 19, pp. 1066–1073, 2011.

[43] D. J. Frew, M. J. Forrestal, and W. Chen, "A split Hopkinson pressure bar technique to determine compressive stress-strain data for rock materials," *Experimental Mechanics*, vol. 41, no. 1, pp. 40–46, 2001.

[44] X. B. Li, T. S. Lok, and J. Zhao, "Dynamic characteristics of granite subjected to intermediate loading rate," *Rock Mechanics and Rock Engineering*, vol. 38, no. 1, pp. 21–39, 2005.

[45] M. Zhang, L. Dou, H. Konietzky, Z. Song, and S. Huang, "Cyclic fatigue characteristics of strong burst-prone coal: experimental insights from energy dissipation, hysteresis and micro-seismicity," *International Journal of Fatigue*, vol. 133, article 105429, 2020.

[46] S. W. Freiman, "Effects of chemical environments on slow crack growth in glasses and ceramics," *Journal of Geophysical Research: Solid Earth*, vol. 89, no. B6, pp. 4072–4076, 1984.

[47] T. A. Michalske and S. W. Freiman, "A molecular interpretation of stress corrosion in silica," *Nature*, vol. 295, no. 5849, pp. 511-512, 1982.

[48] H. Dawei, Z. Hui, H. Qizhi, S. Jianfu, and F. Xiating, "A hydro-mechanical-chemical coupling model for geomaterial with both mechanical and chemical damages considered," *Acta Mechanica Solida Sinica*, vol. 25, pp. 361–376, 2012.

[49] K. Kawai, H. Sakuma, I. Katayama, and K. Tamura, "Frictional characteristics of single and polycrystalline muscovite and influence of fluid chemistry," *Journal of Geophysical Research: Solid Earth*, vol. 120, no. 9, pp. 6209–6218, 2015.

[50] M. O. Ciantia, R. Castellanza, and C. di Prisco, "Experimental study on the water-induced weakening of calcarenites," *Rock Mechanics & Rock Engineering*, vol. 48, no. 2, pp. 441–461, 2015.

[51] M. O. Ciantia, R. Castellanza, G. B. Crosta, and T. Hueckel, "Effects of mineral suspension and dissolution on strength and compressibility of soft carbonate rocks," *Engineering Geology*, vol. 184, pp. 1–18, 2015.

[52] E. Cadoni, K. Labibes, C. Albertini, M. Berra, and M. Giangrasso, "Strain-rate effect on the tensile behaviour of concrete at different relative humidity levels," *Materials and Structures*, vol. 34, no. 1, pp. 21–26, 2001.

[53] P. Rossi, "A physical phenomenon which can explain the mechanical behaviour of concrete under high strain rates," *Materials and Structures*, vol. 24, no. 6, pp. 422–424, 1991.

[54] Z. Zhou, X. Cai, Y. Zhao, L. Chen, C. Xiong, and X. Li, "Strength characteristics of dry and saturated rock at different strain rates," *Transactions of Nonferrous Metals Society of China*, vol. 26, no. 7, pp. 1919–1925, 2016.